

Exploring the impact of under-reported cases on the COVID-19 spatiotemporal distribution using healthcare worker infection data

Peixiao Wang¹, Tao Hu², Hongqiang Liu³ and Xinyan Zhu^{1,4,5,*}

¹ State Key Laboratory of Information Engineering in Surveying, Mapping and Remote Sensing, Wuhan University, Wuhan 430079, China; peixiaowang@whu.edu.cn

² Center for Geographic Analysis, Harvard University, Cambridge, MA 02138, USA; taohu@g.harvard.edu

³ College of Geodesy and Geomatics, Shandong University of Science and Technology, Qingdao 266590, China; liuhongqiang@whu.edu.cn

⁴ Collaborative Innovation Center of Geospatial Technology, Wuhan 430079, China

⁵ Key Laboratory of Aerospace Information Security and Trusted Computing, Ministry of Education, Wuhan University, Wuhan 430079, China

* Correspondence: xinyanzhu@whu.edu.cn

Abstract: A timely understanding of the spatiotemporal pattern and development trend in the early stages of the COVID-19 epidemic were critical for timely prevention and control. However, under-reporting is commonly prevalent in the early stages of an epidemic. In this study, confirmed cases of healthcare workers were considered as accurate small samples to analyze the impact of under-reporting on the spatiotemporal distribution of COVID-19 from three perspectives: parameter estimation, spatiotemporal correlation, and spatiotemporal lag. The results show that (1) the lognormal distribution was the most suitable to describe the evolution of the epidemic with time; (2) the estimated peak infection time of reported cases lagged behind the peak infection time of the healthcare worker cases, and the estimated infection time interval of the reported cases was smaller than that of the healthcare worker cases. (3) The impact of under-reported cases on the early stages of the pandemic was greater than that on its later stages, and the impact on early onset areas was greater than that on late onset areas. (4) Although the number of reported cases was lower than the actual number of cases, a high spatial correlation existed between the cumulatively reported cases and healthcare worker cases.

Keywords: COVID-19; spatiotemporal distribution; healthcare worker infection; under-reporting cases

1 Introduction

Since the outbreak of COVID-19, the prevention and control of the epidemic have rapidly become the focus of social and academic attention (Fang et al., 2020; Guan et al., 2020; Huang et al., 2020). As a new infectious disease, measures such as isolation, restriction of crowd activities, and wearing masks have been the most effective emergency prevention and control measures. To achieve targeted and accurate prevention and control, it is necessary to immediately obtain a timely understanding of the spatiotemporal patterns of the epidemic and determine its development trend (Chen, Li, Gao, Kang, & Shi, 2020).

Data on reported cases have been extremely important in the early stages of the epidemic. Many scholars have used these data to explore the spatiotemporal characteristics of COVID-19,

which includes predicting the inflection point of the disease (Shen, Peng, Xiao, & Zhang, 2020; Tang et al., 2020) and detecting its spatial distribution and movement (Jia et al., 2020; Liu et al., 2020; Wang, Liu, Struthers, & Lian, 2020). However, under-reporting of cases is a very common phenomenon in fields associated with public health, such as epidemiology and biomedicine (Fernández - Fontelo, Cabaña, Puig, & Moriña, 2016). In particular, for newly detected infectious diseases such as COVID-19, under-reporting is more likely to occur due to the lack of understanding of the disease and strict diagnostic criteria (Cabaña, Arratia, Fernández-Fontelo, Moriña, & Puig, 2020).

At present, patient death data are regarded as more accurate and are used to conduct research on the phenomenon of under-reporting in the early stage of COVID-19, such as reconstructing the true epidemic level of COVID-19 and exploring the impact of under-reported cases on the mortality rate and effective reproduction number (Backer, Klinkenberg, & Wallinga, 2020; Golding et al., 2020; Lachmann, Jagodnik, Giorgi, & Ray, 2020; Lau et al., 2020; Linton, Kobayashi, Yang, Hayashi, & Nishiura, 2020; Prado, Antunes, Bastos, Peres, & Bozza, 2020; Saberi et al., 2020). Although the abovementioned studies analyzed the impact of under-reporting on the epidemic situation from multiple perspectives, some discrepancies still remain. First, death data still need to be accurately reported, and there may be a deviation between the number of reported deaths and the actual number of deaths due to COVID-19. Secondly, few studies have explored the impact of under-reported cases on the spatiotemporal distributions of COVID-19.

Compared with patient death data, information on healthcare workers with COVID-19 can be considered as a more accurate due to the smaller dataset. In the early stage of the epidemic, healthcare worker infections were more easily detected and calculated. Therefore, data on confirmed cases of healthcare workers can more accurately reflect the relevant characteristics of COVID-19 (Gao, Sanna, Tsai, & Wen, 2020). Additionally, it is common to estimate population characteristics using small samples in the field of statistics (Lauer et al., 2020; Mace, Minta, Manley, & Aune, 1994; Smid, McNeish, Miočević, & van de Schoot, 2020). For example, Li et al. (2020) estimated the infection peak time via data on reported cases as well as via an internet search and social media data. Backer et al. (2020) and Linton et al. (2020) estimated the incubation period of COVID-19 via a small number of reported cases. However, these studies only estimated the temporal characteristics of COVID-19.

Considering this, data on confirmed cases of healthcare workers were used in this study to analyze the impact of under-reported cases from a spatiotemporal perspective to provide scientific support for researchers. The main contributions of this article are as follows:

- (1) A novel data source, healthcare workers infection data, was used for analyzing the impact of under-reported cases on the spatiotemporal distribution of COVID-19.
- (2) Analysis methods were extended, i.e., we not only analyzed the impact of under-reported cases on the temporal characteristics, but also the impact on spatial characteristics from the perspective of spatial correlation and lag.
- (3) The research framework of this paper is highly extensible, and researchers can use other data sources to carry out similar research.

2 Study Area and Data Sources

User ID	Date	Province	City	County
1	2020-01-15	Hubei	Wuhan	Huangpo
2	2020-01-15	Hubei	Jingmen	Zhongxiang
3	2020-02-04	Shandong	Qingdao	Shinan
.....
3743	2020-02-01	Beijing	Beijing	Xicheng

2.2.2 Data Preprocessing

Data on reported cases were collected and processed at the China Data Center and shared on the dataverse platform of Harvard University, which does not require additional data preprocessing (Hu et al., 2020; Yang et al., 2020). Therefore, we mainly conducted data preprocessing for information on healthcare workers suffering from COVID-19, which was obtained via retrospective analyses.

The information on healthcare workers obtained via retrospective analyses is mainly reported to the Chinese Red Cross Foundation in two ways (Foundation, 2020): (1) confirmed information on healthcare workers is directly reported by individuals to the Chinese Red Cross Foundation; and (2) confirmed information on healthcare workers is collected by their respective hospitals, which then report to the Chinese Red Cross Foundation. After examination and approval by the Chinese Red Cross Foundation, the relevant information is published on the website after which the hospital may review it. Those who fail to pass the review do not qualify to be aided. Therefore, data records of unqualified persons should be deleted from the original data. Moreover, the Chinese Red Cross Foundation not only aided infected healthcare workers, but also infected or diseased staff during the epidemic. Thus, such data records needed to be deleted. As shown in Figure 2a, after data preprocessing, a total of 3,703 confirmed cases of healthcare workers remained, including 3,655 from Hubei Province and 3,058 from Wuhan City. Compared with real-time data on the confirmed COVID-19 cases of healthcare workers in the same period (Figure 2b) (Epidemiology Working Group for NCIP Epidemic Response, 2020; Gao et al., 2020), the corresponding data obtained via retrospective analyses exhibited an obvious quantitative advantage.

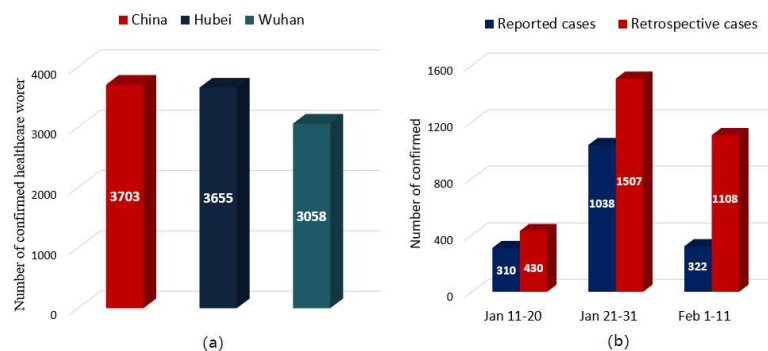


Figure 2. Characteristics of healthcare worker infection data. (a) Number of confirmed healthcare workers and (b) number of confirmed cases.

3 Methods

In this study, data on confirmed cases of healthcare workers were considered to represent an accurate and small sample space to explore the impact of under-reporting on the spatiotemporal distribution of COVID-19. The overall framework is shown in Figure 3. First, infection inventories were constructed for the healthcare workers and reported cases in Hubei and Wuhan. Second, based on these inventories, the impacts of under-reported cases on the temporal characteristics were analyzed from three perspectives, namely parameter estimation, temporal correlation, and temporal lag. Finally, the impacts of under-reported cases on the spatial characteristics were analyzed from the perspective of spatial correlation and spatial lag. This work provides scientific support for researchers that explore the spatiotemporal distribution of COVID-19 using the on reported cases.

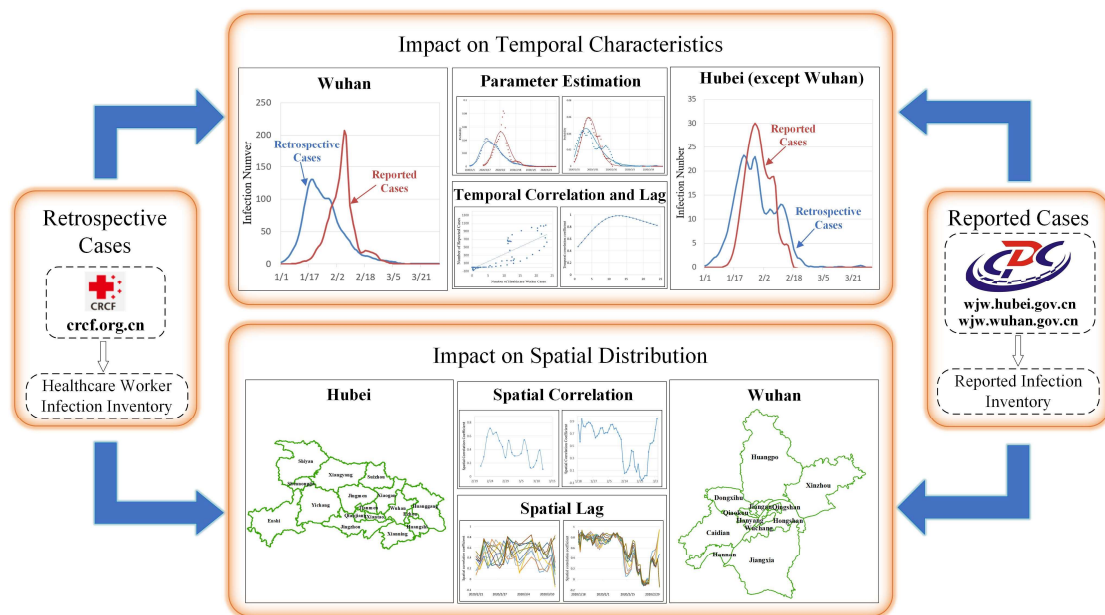


Figure 3. Research framework for investigating the impact of under-reported cases on the spatiotemporal distribution of COVID-19

3.1 Construction of Infection Inventory

Due to the incubation time of the SARS-COV-2 infection, the confirmed time does not represent the infection time of the healthcare workers and reported cases. Therefore, this study constructed a *Healthcare Worker Infection Inventory* and a *Reported Infection Inventory* based on partition statistics for two regions: Hubei and Wuhan.

The construction of the *Infection Inventory* was divided into two steps: (1) Generate a *Confirmed Inventory* based on confirmed healthcare worker data, and (2) Generate an *Infection Inventory* based on the *Confirmed Inventory*. The data structures for the two inventories are shown in Figure 4. $Inventory(S, T)$ represents a spatiotemporal dataset, where S and T are the spatial and temporal dimension, respectively; $S = \{s_1, s_2, \dots, s_m\}$, $T = \{t_1, t_2, \dots, t_n\}$, m is the total number of spatial objects and n is the total number of timestamps.

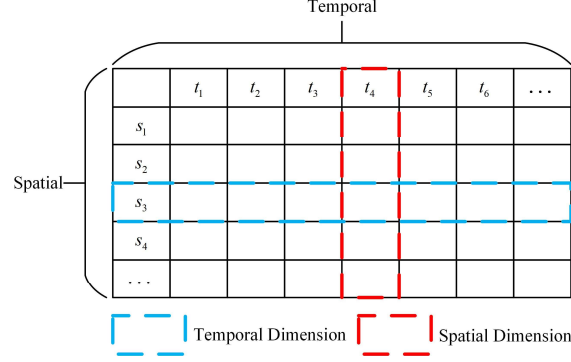


Figure 4. Data structure of the confirmed and infection inventories.

Considering the healthcare workers in Wuhan as an example, to construct the *Healthcare Worker Infection Inventory* in Wuhan, the *Confirmed Healthcare Worker Inventory* in Wuhan City was first generated. For example, the calculation method for the number of confirmed healthcare workers on day t_0 in Hongshan, Wuhan City, is shown in Equation (1):

$$\left\{ \begin{array}{l} H_C_Inventory^{Wuhan}(Hongshan, t_0) = \sum_i^N |cms_i. County == Hongshan \wedge cms_i. Date == t_0| \\ cms_i \in Retrospective\ Healthcare\ Worker\ Infection\ Set \end{array} \right. \quad (1)$$

where N represents the total number of confirmed healthcare worker infections in China, cms_i represents the information of a specific healthcare worker suffering from COVID-19, and $H_C_Inventory^{Wuhan}$ represents the *Confirmed Healthcare Worker Inventory* in Wuhan, which elucidates the changes in confirmed healthcare worker infections in every county of Wuhan over time.

To calculate the *Healthcare Worker Infection Inventory*, we assumed that the incubation time X of SARS-Cov-2 is subject to a lognormal distribution, as seen in other acute respiratory viral infections (Justin et al., 2009). Lauer et al. (2020) found that the mean and standard deviation of the random variable $\ln(X)$ were 1.621 and 0.418, respectively, i.e., $\ln(X) \sim N(1.621, 0.418^2)$. Based on the probability distribution function of the incubation time X , the daily infected number of healthcare workers can be calculated. For example, the calculation method for the infected number of healthcare workers on day t_0 in Hongshan, Wuhan City, is shown in Equation (2):

$$\left\{ \begin{array}{l} H_I_Inventory^{Wuhan}(Hongshan, t_0) = \sum_i^n H_C_Inventory^{Wuhan}(Hongshan, t_0 + i) * p_i \\ p_i = \int_{\ln(i-1)}^{\ln(i)} \frac{1}{\sqrt{2\pi}\sigma} e^{-\frac{(x-u)^2}{2\sigma^2}} \quad i.e., 1 < i < 13 \\ p_i = (1 - \sum_2^{12} p_j)/2 \quad i.e., i = 1 \text{ or } i = 13 \end{array} \right. \quad (2)$$

where p_i represents the probability that the incubation time is i days; n represents the maximum incubation time (as the incubation time of 98.7% patients is within 13 days, n is set as 13); u represents the mean of the log normal distribution, i.e., 1.621; σ represents the standard deviation of the log normal distribution, i.e., 0.418; and $H_I_Inventory^{Wuhan}$ represents the *Healthcare Worker Infection Inventory* in Wuhan. Similarly, the *Reported Infection Inventory* in Wuhan can be expressed as $R_I_Inventory^{Wuhan}$, and the corresponding *Healthcare Worker Infection Inventory* and *Reported Infection Inventory* in Hubei can be expressed as

$H_I_Inventory^{Hubei}$ and $R_I_Inventory^{Hubei}$, respectively. Taking Hubei Province as an example, Tables 2 and 3 show further details of the *Reported Infection Inventory* and *Healthcare Worker Infection Inventory*.

Table 2. Sample of *Reported Infection Inventory* in Hubei

	2020-01-24	2020-01-25	2020-01-26	2020-01-27	2020-01-28
Wuhan	591	676	839	1033	1268
Ezhou	40	43	44	43	42
Huanggang	141	160	175	191	200
.....
Suizhou	59	71	81	90	94

Table 3. Sample of *Healthcare Worker Infection Inventory* in Hubei

	2020-01-24	2020-01-25	2020-01-26	2020-01-27	2020-01-28
Wuhan	106	102	100	101	101
Ezhou	5	5	5	4	4
Huanggang	5	4	5	5	6
.....
Suizhou	1	1	1	1	2

3.2 Statistical Model

The T in $Inventory(S, T)$ is essentially a collection of time-series data, which record the temporal characteristics of healthcare worker infection. Studies have shown that counts of the less frequent infections typically follow a Poisson distribution, whereas those of more frequent infections may follow approximately a normal distribution (Farrington, Andrews, Beale, & Catchpole, 1996; Unkel, Farrington, Garthwaite, Robertson, & Andrews, 2012). In the early stages of the epidemic, SARS-Cov-2 infections were frequent. Therefore, two samples of healthcare worker cases and reported cases were used to estimate the infection peak time and the infection time interval of the epidemic based on three distributions: normal, log normal, and gamma. The probability density function of normal, log normal, and gamma are shown in Equations (3), (4), and (5), respectively:

$$Normal(x; u, \sigma) = \frac{1}{\sqrt{2\pi}\sigma} e^{\left(-\frac{(x-u)^2}{2\sigma^2}\right)}, \quad (3)$$

$$Lognormal(x; u_l, \sigma_l) = \frac{1}{\sqrt{2\pi}\sigma_l} e^{\left(-\frac{(\ln x - u_l)^2}{2\sigma_l^2}\right)}, \quad (4)$$

$$Gamma(x; \alpha, \beta) = \frac{\beta^\alpha}{\Gamma(\alpha)} x^{\alpha-1} e^{-\beta x}, \quad (5)$$

where u and σ represent the fixed parameters of the normal, u_l and σ_l represent the fixed parameters of the log normal, α and β represent the fixed parameters of the gamma distribution, and $\Gamma(\alpha)$ represents the gamma function. In this study, maximum likelihood estimation was used to fit the hyper parameters of the three distributions. As gamma and log

normal distributions are skewed, the median of the distributions was used to approximate the peak time of infection.

In addition, the cumulative distribution functions of the normal, log normal, and gamma distributions were used to estimate the time interval of the infection. For example, the calculation method of the infection time interval for the normal distribution is shown in Equation (6) as follows:

$$\left\{ \begin{array}{l} \text{infection time interval} = [\underline{x}, \bar{x}] \\ \underline{x} = F_{normal}^{-1}(0.025) \\ \bar{x} = F_{normal}^{-1}(0.975) \\ F_{normal}(x) = \int_{-\infty}^x Normal(t)dt \end{array} \right. \quad (6)$$

where $F_{normal}(x)$ represents the cumulative distribution functions of the normal, $F_{normal}^{-1}(x)$ represents the inverse function of $F_{normal}(x)$, \underline{x} represents the lower bound of the interval, and \bar{x} represents the upper bound of the interval. That is, the infection time interval represents the time span of an epidemic infection in 95% of patients. In this study, when the difference between the infection peak and infection interval estimated based on the two samples was small, under-reported cases had less impact on the temporal characteristics, and vice versa.

3.3 Pearson Correlation Coefficient

The Pearson correlation coefficient is used to measure the degree of correlation between two series (Benesty, Chen, Huang, & Cohen, 2009). As $Inventory(S, T)$ contains both temporal and spatial dimensions, we calculated temporal and spatial correlations. As shown in Figure 5, the spatial correlation was obtained by h_{i_t3} and r_{i_t3} , and the temporal correlation was obtained by h_{i_s3} and r_{i_s3} . The temporal and spatial correlation coefficients of the two series were calculated using Equations (7) and (8), respectively:

$$r_{temporal} = \frac{Cov(h_{i_s_i}, r_{i_s_i})}{\sqrt{D(h_{i_s_i})}\sqrt{D(r_{i_s_i})}} \quad (7)$$

$$r_{spatial} = \frac{Cov(h_{i_t_i}, r_{i_t_i})}{\sqrt{D(h_{i_t_i})}\sqrt{D(r_{i_t_i})}} \quad (8)$$

where $h_{i_s_i}$ represents the time series of healthcare worker infections in a specific spatial region, $r_{i_s_i}$ represents the time series of reported infections in a specific spatial region, $h_{i_t_i}$ represents the spatial series of healthcare worker infections during a specific time, and $r_{i_t_i}$ represents the spatial series of reported infections during a specific time. $Cov(X, Y)$ represents the covariance of series X and Y , $D(X)$ represents the variance of series X , and $\sqrt{D(X)}$ represents the standard deviation of series X . The value range of the correlation coefficient is $[-1, 1]$. When the correlation coefficient is greater than 0, time series X and Y are positively correlated; if it is equal to 1, time series X and Y are completely positively correlated; if it is less than 0, time series X and Y show a negative correlation; and finally, if it is equal to -1, time series X and Y show a completely negative correlation. In this study, if the two series showed a significant positive correlation, the under-reporting of cases had less impact on the spatiotemporal characteristics, and vice versa.

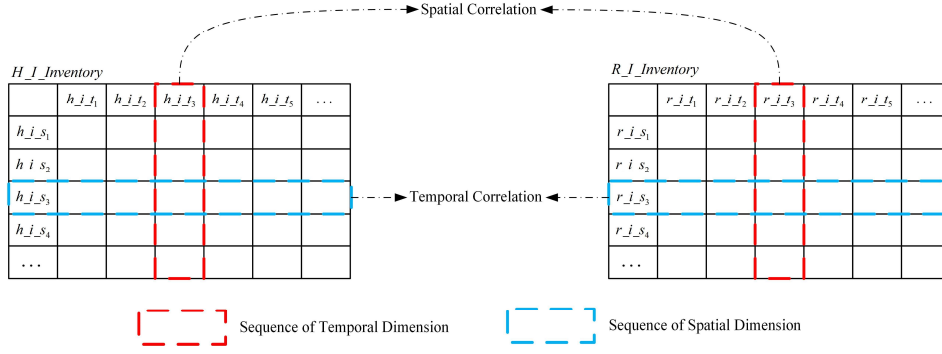


Figure 5. Temporal and spatial correlation coefficients

3.4 Cross-correlation Function

The cross-correlation function measures the impact of under-reported cases on the spatiotemporal characteristics based on a lag. As shown in Figure 6, the cross-correlation function can be understood as a correlation coefficient with a lag (Derrick & Thomas, 2004).

With regard to the spatial dimension, the spatial lag of series h_{i,t_i} and r_{i,t_i} was calculated using Equation (9), as follows:

$$f_{spatial}(\varphi) = \frac{Cov(h_{i,t_{i+\varphi}}, r_{i,t_i})}{\sqrt{D(h_{i,t_{i+\varphi}})}\sqrt{D(r_{i,t_i})}} \quad (9)$$

where $f_{spatial}(\varphi)$ is the spatial correlation coefficient between series $h_{i,t_{i+\varphi}}$ and r_{i,t_i} at lag φ , r_{i,t_i} represents the spatial series of reported infections during a specific time, $h_{i,t_{i+\varphi}}$ represents the spatial series of healthcare worker infections lagging behind φ days compared to time i .

With regards to the temporal dimension, the temporal lag of series $h_{i,s_i} = \{h_{i,s_i^t}\}_{t=1}^n$ and $r_{i,s_i} = \{r_{i,s_i^t}\}_{t=1}^n$ was calculated using Equation (10), as follows:

$$\begin{cases} f_{temporal}(\varphi) = \frac{\gamma_{temporal}(\varphi)}{\sqrt{\sigma_{h_{i,s_i}}}\sqrt{\sigma_{r_{i,s_i}}}} \\ \gamma_{temporal}(\varphi) = E \left[(h_{i,s_i^t} - \bar{h}_{i,s_i^t}) (r_{i,s_i^{t+\varphi}} - \bar{r}_{i,s_i^{t+\varphi}}) \right] \end{cases} \quad (10)$$

where $f_{temporal}(\varphi)$ is the temporal correlation coefficient between series h_{i,s_i} and r_{i,s_i} at lag φ , h_{i,s_i^t} represents the time series of healthcare worker infections in a specific spatial region, $r_{i,s_i^{t+\varphi}}$ represents the time series of reported infections lagging behind φ days compared to time i in a specific spatial region.

In the definition, the cross-correlation function can be regarded as a function of the lag, and the lag value that maximizes the cross-correlation function is the average delay time of the actual infection. The formal definition can be seen in Equation (11):

$$\begin{cases} \hat{\varphi}_{temporal} = \operatorname{argmax}(f_{temporal}(\varphi)) \\ \hat{\varphi}_{spatial} = \operatorname{argmax}(f_{spatial}(\varphi)) \end{cases} \quad (11)$$

where $\hat{\varphi}_{spatial}$ represents the estimated delay in space, $\hat{\varphi}_{temporal}$ represents the estimated delay in time, and the mean of $f_{temporal}(\varphi)$ and $f_{spatial}(\varphi)$ are the same as those in Equations (9) and (10). The smaller $\hat{\varphi}$, the smaller the impact of under-reported cases on the spatiotemporal characteristics, and vice versa.

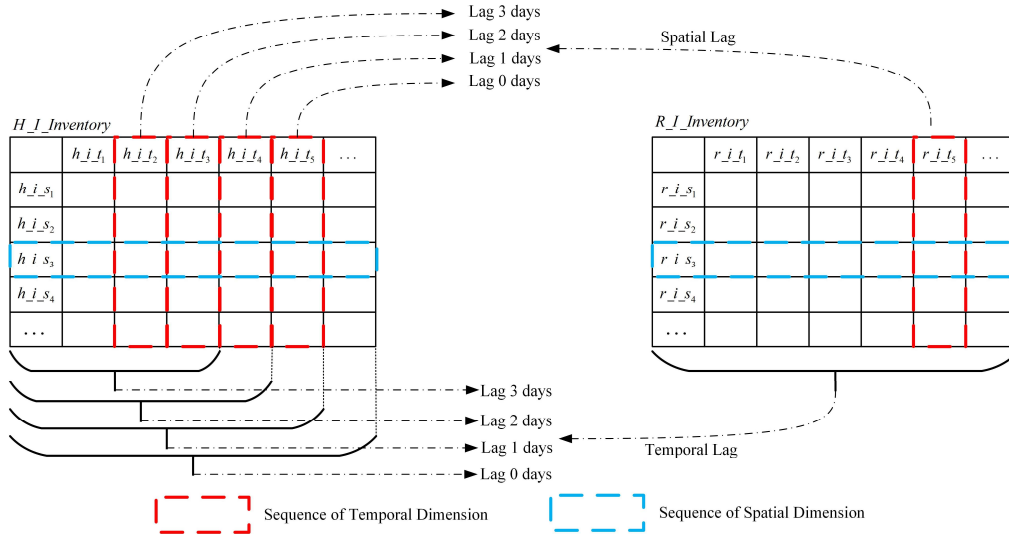


Figure 6. Temporal and spatial lag

4 Experimental Results and Analysis

4.1 Impact of Under-reported Cases on Temporal Characteristics

To analyze the impact of under-reported cases on the temporal characteristics of COVID-19, we first used the data on reported cases and confirmed healthcare worker infections to estimate the epidemic peak and infection interval in Wuhan and Hubei (except Wuhan). Then, we further analyzed the temporal correlation and temporal lag of the data on reported cases and confirmed healthcare worker infections in Wuhan and Hubei (except Wuhan).

4.1.1 Impact of Under-reported Cases on Infection Peak and Interval

Figure 7 shows the fitting results of normal, log normal, and gamma distributions for healthcare worker cases and reported cases in Wuhan, and the mean square error (MSE) was used to evaluate the fitting effect of each distribution. The results showed that the MSE of the log normal distribution was the lowest, which indicated that this distribution was the most suitable to describe the evolution of the epidemic with time in Wuhan. In addition, Tables 4 and 5 show the statistical characteristics of healthcare worker cases and reported cases in Wuhan. According to the log normal distribution, the peak time of infection in Wuhan estimated from the data on daily reported cases was on February 3. However, from the data on daily healthcare worker infection cases, it was estimated to be on January 24, i.e., a difference of 11 days. The standard deviation estimated from daily reported cases was 7.6 days; 95% of the patients in Wuhan were infected from January 21 to February 19, i.e., within 30.0 days. However, the standard deviation estimated by the daily healthcare worker infection cases was 10.6 days; therefore, 95% of the patients in Wuhan were more likely to be infected from January 8 to February 22, i.e., within 45.6 days.

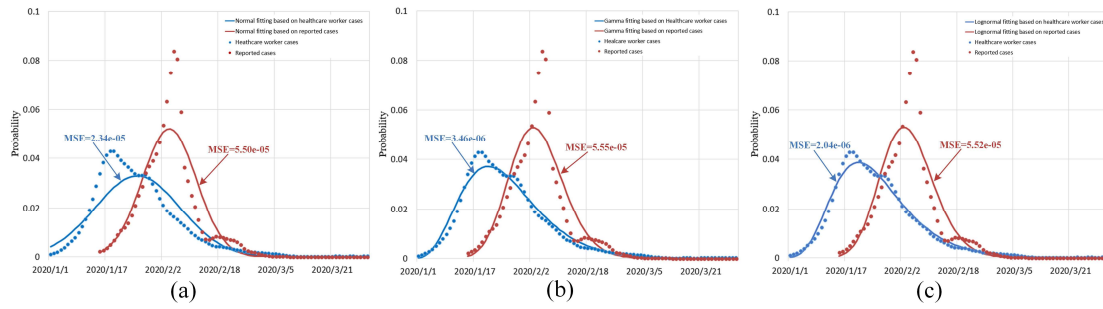


Figure 7. Fitting results of statistical distributions for healthcare worker cases and reported cases in Wuhan: (a) normal distribution, (b) gamma distribution, and (c) log normal distribution.

Table 4. Estimated results of the median and standard deviation for healthcare worker cases and reported cases in Wuhan

Distribution		Median (peak)		Standard Deviation (days)	
		Healthcare workers cases	Reported cases	Healthcare workers cases	Reported cases
Normal	Estimate	Jan 25	Feb 3	12.1 days	7.6 days
	95% CI	Jan 24–Jan 26	Feb 3–Feb 4	10.8 days–13.5 days	7.4 days–8.0 days
Lognormal	Estimate	Jan 23	Feb 3	11.8 days	7.6 days
	95% CI	Jan 23–Jan 24	Feb 2–Feb 3	11.2 days–12.3 days	7.4 days–7.9 days
Gamma	Estimate	Jan 24	Feb 3	11.6 days	7.6 days
	95% CI	Jan 23–Jan 24	Feb 3–Feb 4	11.1 days–12.1 days	7.4 days–7.9 days

Table 5. Estimated results of percentiles and infection time intervals of healthcare worker cases and reported cases in Wuhan

Percentiles		Healthcare workers cases			Reported cases		
		Normal	Lognormal	Gamma	Normal	Lognormal	Gamma
2.5 th	Estimate	Jan 1	Jan 8	Jan 7	Jan 19	Jan 21	Jan 20
	95% CI	Dec 30–Jan 4	Jan 5–Jan 9	Jan 6–Jan 8	Jan 18–Jan 20	Jan 19–Jan 22	Jan 19–Jan 22
97.5 th	Estimate	Feb 18	Feb 22	Feb 21	Feb 18	Feb 19	Feb 19
	95% CI	Feb 15–Feb 21	Feb 20–Feb 25	Feb 18–Feb 25	Feb 17–Feb 20	Feb 18–Feb 21	Feb 18–Feb 21
Infection time interval	Estimate	47.5 days	45.6 days	45.0 days	30.1 days	30.0 days	30.0 days
	95% CI	40.6 days–55.0 days	42.6 days–49.7 days	40.8 days–49.1 days	27.6 days–32.3 days	27.5 days–32.4 days	27.5 days–32.0 days

Figure 8 shows the scattered distributions for healthcare worker cases and reported cases in Hubei (excluding Wuhan). From the scatter of healthcare worker cases, the distribution of the epidemic should have been fitted in two segments. However, by reporting case data, we believe that there were not two epidemic peaks, but rather policy reasons that changed the trend of infection among healthcare workers. Therefore, we only used a single curve to fit the distribution. The results showed that the MSE of the log normal and gamma distributions was relatively small. In addition, Tables 6 and 7 show the statistical characteristics of healthcare worker cases and reported cases in Hubei (excluding Wuhan). Compared with Wuhan, the impact of under-reported cases on the temporal characteristics of the epidemic in Hubei

(excluding Wuhan) was relatively small. According to the log normal distribution, the peak time of infection in Hubei (except Wuhan) estimated from the data on daily reported cases was January 28, whereas that estimated from the data on daily healthcare worker infection cases was February 29, i.e., only differing by one day. The standard deviation estimated from the daily reported cases was 6.8 days. Furthermore, 95% of the patients in Hubei (excluding Wuhan) were infected from January 17 to February 12, i.e., within 23.7 days. The standard deviation estimated by the daily healthcare worker infection cases was 10.2 days, and therefore, 95% of the patients in Hubei (excluding Wuhan) were more likely to be infected from January 15 to February 23, i.e., within 39.3 days.

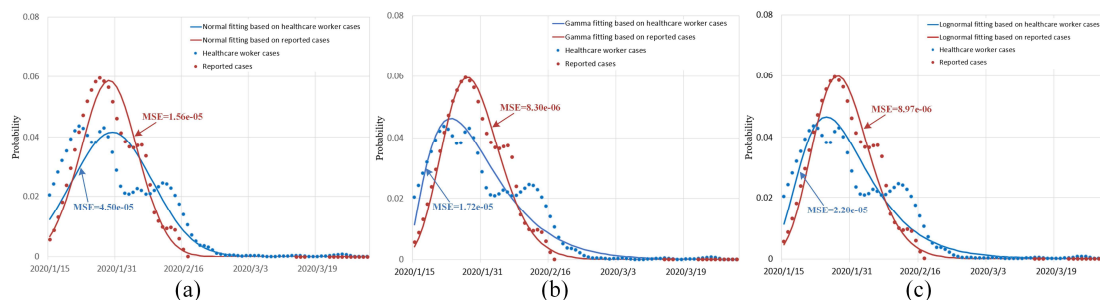


Figure 8. Fitting results of statistical distributions for healthcare worker cases and reported cases in Hubei (excluding Wuhan): (a) normal distribution, (b) gamma distribution, and (c) log normal distribution.

Table 6. Estimated results of the median and standard deviation for healthcare worker cases and reported cases in Hubei (excluding Wuhan)

Distribution		Median (peak)		Standard Deviation	
		Healthcare workers cases	Reported cases	Healthcare workers cases	Reported cases
Normal	Estimate	Jan 29	Jan 29	9.6 days	6.8 days
	95% CI	Jan 29–Jan 30	Jan 28–Jan 29	9.2 days–10.0 days	6.4 days–7.1 days
Lognormal	Estimate	Jan 28	Jan 29	10.2 days	6.8 days
	95% CI	Jan 27–Jan 29	Jan 27–Jan 29	9.6 days–10.9 days	6.4 days–7.2 days
Gamma	Estimate	Jan 28	Jan 28	10.4 days	6.9 days
	95% CI	Jan 26–Jan 28	Jan 27–Jan 29	9.7 days–11.0 days	6.4 days–7.2 days

Table 7. Estimated results of percentiles and infection time intervals for healthcare worker cases and reported cases in Hubei (excluding Wuhan)

Percentiles		Healthcare workers cases			Reported cases		
		Normal	Lognormal	Gamma	Normal	Lognormal	Gamma
2.5 th	Estimate	Jan 11	Jan 15	Jan 16	Jan 15	Jan 17	Jan 17
	95% CI	Jan 10–Jan 12	Jan 14–Jan 16	Jan 15–Jan 16	Jan 14–Jan 16	Jan 16–Jan 18	Jan 16–Jan 18
97.5 th	Estimate	Feb 17	Feb 23	Feb 24	Feb 11	Feb 12	Feb 13
	95% CI	Feb 16–Feb 19	Feb 21–Feb 26	Feb 22–Feb 26	Feb 10–Feb 12	Feb 11–Feb 14	Feb 11–Feb 14
Infection time interval	Estimate	37.6 days	39.3 days	39.3 days	26.7 days	26.7 days	26.7 days
	95% CI	35.5 days–39.5 days	36.8 days–41.9 days	36.7 days–42.1 days	25.1 days–28.0 days	25.1 days–28.1 days	25.1 days–28.1 days

In general, when the phenomenon of under-reporting is not considered, the infection peak and infection interval estimated by reported cases may be significantly different from the actual infection peak and infection interval. Among them, the estimated infection peak time may be earlier than the actual infection peak time, and the estimated infection time interval may be smaller than the actual infection time interval. In addition, the impact of the under-reporting phenomenon in Wuhan was greater than that on Hubei (excluding Wuhan).

4.1.2 Impact of Under-reported Cases on Temporal Correlation

Figure 9 shows the temporal correlation between the confirmed healthcare worker cases and the reported cases in Wuhan. The temporal correlation coefficient between the data on daily reported cases and new healthcare worker cases in Wuhan was 0.336, which indicated that the temporal correlation between daily reported cases and actual infection cases was weak. The correlation coefficient between the cumulative reported cases and the cumulative healthcare worker cases in Wuhan was 0.926. As shown in Figure 9d, although there was a strong temporal correlation between the cumulative reported cases and actual infection cases in Wuhan, the distance between the trend line and the scatter points was still large in the early stage of the epidemic. This indicated that the temporal correlation gradually increased over time, so that the phenomenon of under-reporting gradually decreased over time.

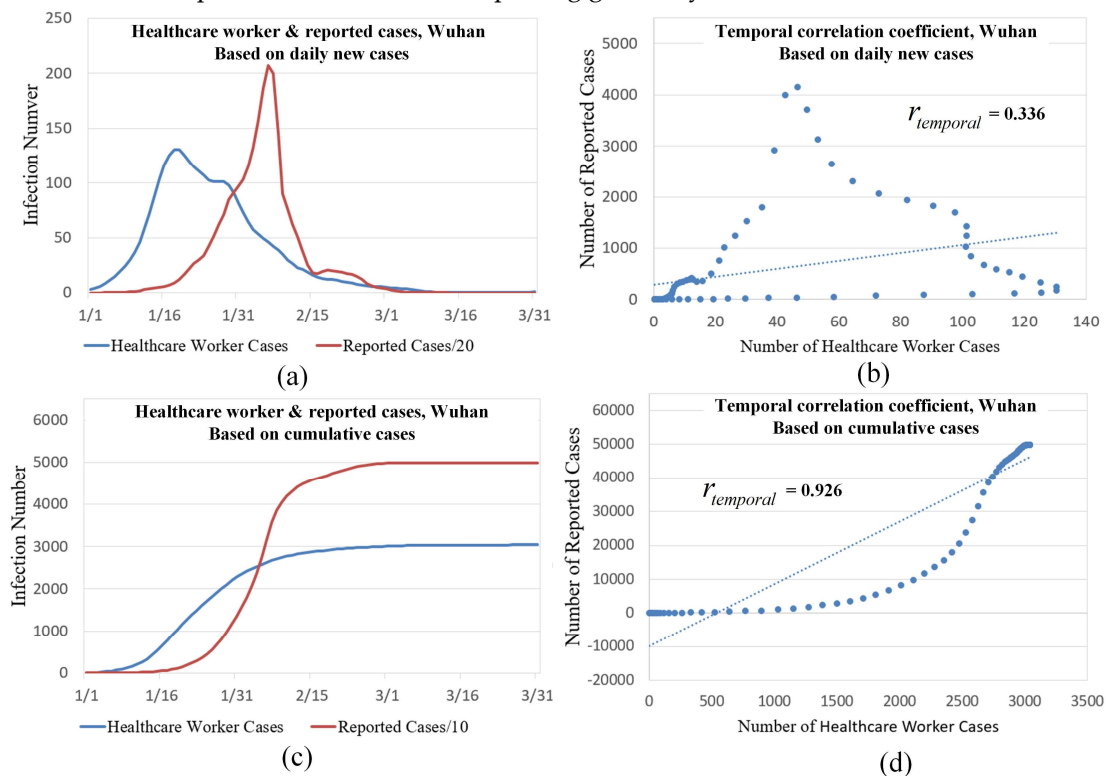


Figure 9. Temporal differences between healthcare worker cases and reported cases in Wuhan. (a) Healthcare worker and reported cases in Wuhan, based on daily new cases; (b) temporal correlation coefficient in Wuhan, based on daily new cases; (c) healthcare worker and reported cases in Wuhan, based on cumulative cases; and (d) temporal correlation coefficient in Wuhan, based on cumulative cases.

Figure 10 shows the temporal correlation between the confirmed healthcare worker cases

and the reported cases in Hubei (except Wuhan). Compared with the temporal correlation coefficient in Wuhan, that in Hubei (excluding Wuhan) was significantly higher. For example, the correlation coefficient between the daily reported cases and new healthcare worker cases in Hubei (excluding Wuhan) was 0.828, which indicated that the temporal correlation between daily reported cases and actual infection cases was relatively strong (excluding Wuhan). In addition, the correlation coefficient between the cumulative reported cases and the cumulative healthcare worker cases in Wuhan was 0.988, and the scattered points were mostly around the trend line. This indicated that the impact of under-reported cases in Hubei (excluding Wuhan) was relatively small.

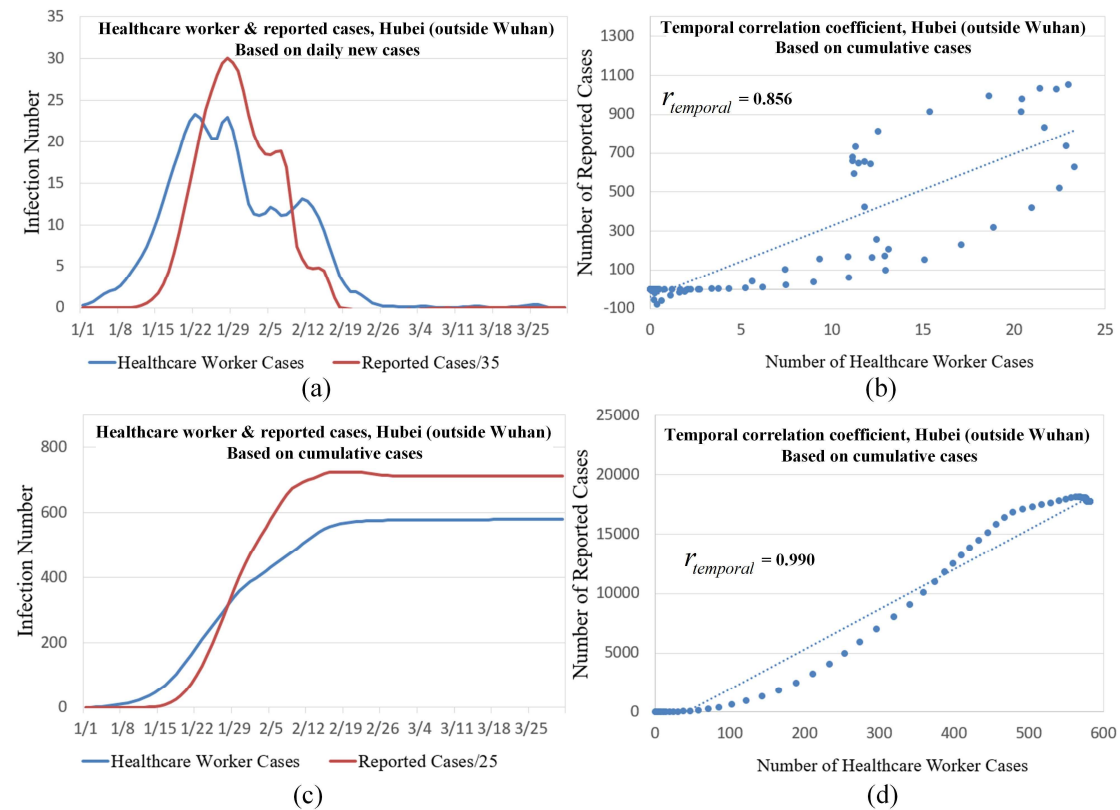


Figure 10. Temporal differences between healthcare worker cases and reported cases in Hubei (excluding Wuhan). (a) Healthcare worker and reported cases in Hubei (excluding Wuhan), based on daily new cases; (b) temporal correlation coefficient in Hubei (excluding Wuhan), based on daily new cases; (c) healthcare worker and reported cases in Hubei (excluding Wuhan), based on cumulative cases; and (d) temporal correlation coefficient in Hubei (excluding Wuhan), based on cumulative cases.

4.1.2 Impact of Under-reported Cases on Temporal Lag

According to Figures 9 and 10, if the phenomenon of under-reporting is not considered, the estimated peak time of infection in the reported cases may lead to a time lag. Therefore, we quantitatively analyzed the time lag in Wuhan and Hubei (excluding Wuhan). Figure 11 shows the time-lag results of the healthcare worker infection cases and reported cases in Wuhan and Hubei (excluding Wuhan). With the increase in φ , the autocorrelation function showed an increasing and then a decreasing trend, revealing a certain lag in the temporal characteristics in Wuhan and Hubei (excluding Wuhan). When $\hat{\varphi} = 13$ days, the autocorrelation function of

Wuhan had the maximum value, and the correlation coefficient between the daily reported cases and new healthcare worker cases was 0.984. When $\hat{\varphi} = 3$ days, the autocorrelation function of Hubei (excluding Wuhan) had the maximum value, and the correlation coefficient between the daily reported cases and new healthcare worker cases was 0.972.

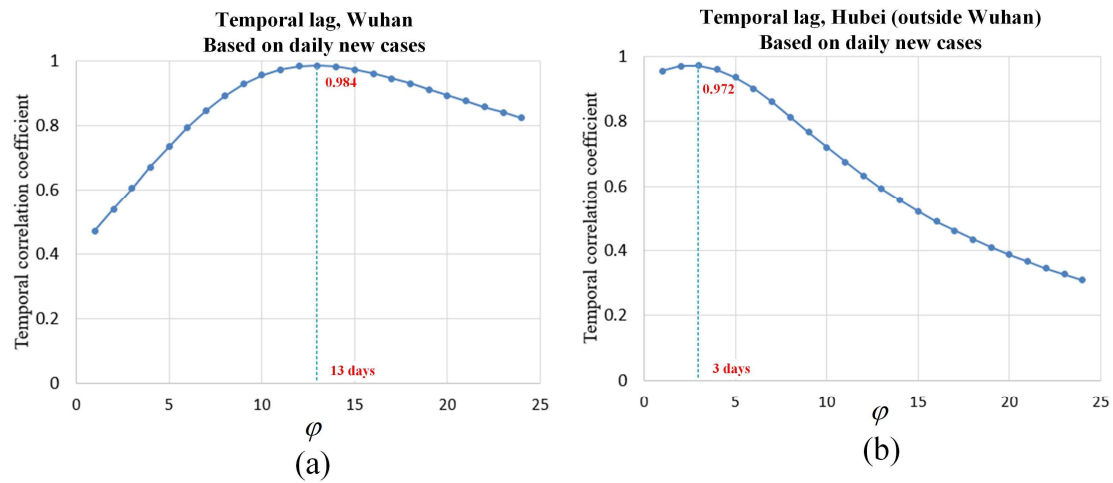


Figure 11. Temporal lag between the healthcare worker cases and under-reported cases: (a) Wuhan City and (b) Hubei Province (excluding Wuhan).

In addition, we further quantitatively analyzed the time lag phenomenon of the counties in Wuhan and the cities in Hubei (excluding Wuhan). In Hubei, we calculated the time lag in cities where the cumulative number of healthcare worker infections exceeded 10. In Wuhan, we calculated the time lag in counties that still reported daily cases after February 21. Figure 12 shows that the time lag phenomenon was spatially heterogeneous in Wuhan and Hubei (excluding Wuhan). Regarding the spatial scale of Hubei, the closer to Wuhan, the greater the time lag; for example, the time lag in areas around Wuhan were up to 8 days. Regarding the spatial scale of Wuhan, the time lag near the city center was larger, as the central area of Wuhan was the most affected region with regard to the number of cases.

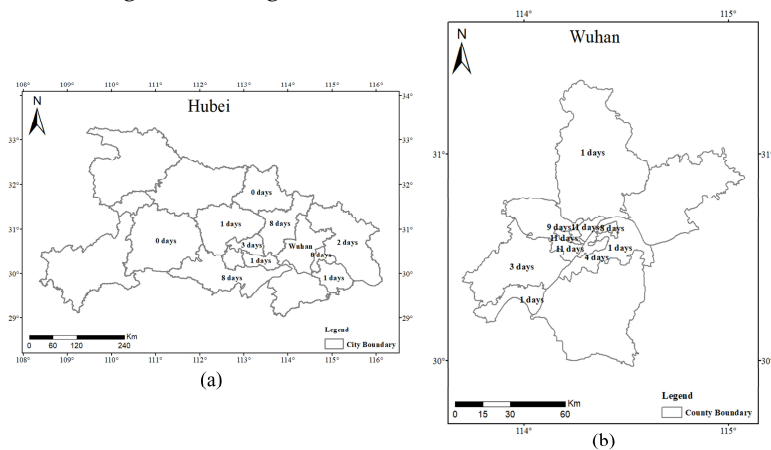


Figure 12. Temporal lag of the counties in Wuhan and the cities in Hubei (excluding Wuhan): (a) Wuhan City and (b) Hubei Province (excluding Wuhan).

In general, the phenomenon of under-reporting had a great impact on the estimated temporal characteristics of the epidemic, and the impact in Wuhan was greater than that in Hubei (excluding Wuhan). According to the time of the occurrence of the epidemic in different regions, the impact of under-reporting in the early onset area was greater than that in the late

onset area, and the impact in the early stage was greater than that in the later stage.

4.2 Impact of Under-reported Cases on Spatial Characteristics

To analyze the impact of under-reported cases on the spatial characteristics of COVID-19, we first analyzed the spatial distribution and spatial correlation of the data on reported cases and confirmed healthcare worker infections on a single time node in Wuhan and Hubei (excluding Wuhan). Then, the spatial lag of the data on reported cases and confirmed healthcare worker infections was further analyzed in Wuhan and Hubei (excluding Wuhan).

4.2.1 Impact of Under-reported Cases on Spatial Correlation

Figure 13 shows the spatial distribution and spatial correlation of the healthcare worker infections and reported cases in Wuhan on March 6. According to Figure 7a and 7b, except for the Jiangxia District, the spatial distribution of healthcare worker infections and reported cases in Wuhan was quite similar, which indicates that, although the level of reported cases was less than the number of actual cases, the spatial distribution of reported cases still reflected the spatial distribution of COVID-19. Moreover, the spatial correlation coefficient between newly reported cases and the healthcare worker cases was 0.544 in Wuhan on March 6, whereas that between the cumulative reported cases and the healthcare worker cases was 0.889. These results show that there was a certain deviation between the newly reported and healthcare worker cases in Wuhan on March 6; however, there was a high correlation between the cumulative reported cases and healthcare worker cases, which implied that the phenomenon of under-reporting had little impact on the spatial distribution of COVID-19 in Wuhan.

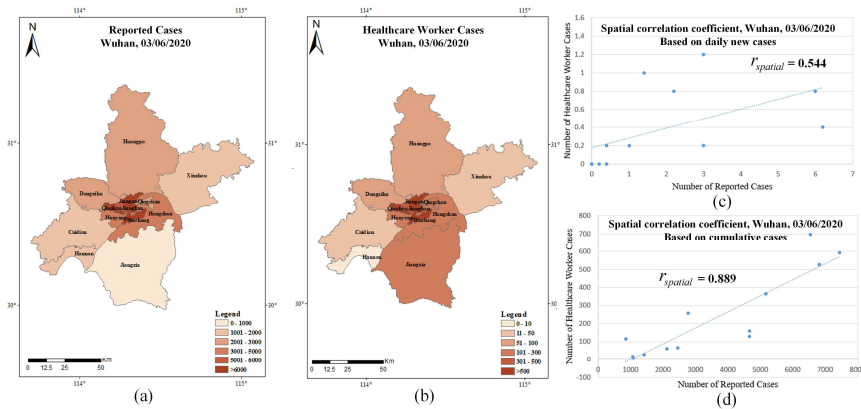


Figure 13. Spatial correlations between healthcare worker cases and reported cases in Wuhan. (a) Reported cases in Wuhan on March 6, 2020; (b) healthcare worker cases in Wuhan on March 6, 2020; (c) spatial correlation coefficient in Wuhan on March 6, 2020, based on daily new cases; and (d) spatial correlation coefficient in Wuhan on March 6, 2020, based on cumulative cases

Figure 14 shows the spatial distribution and spatial correlation of healthcare worker and reported cases in Hubei (excluding Wuhan) on February 6. Compared with Wuhan, the spatial distributions of healthcare worker and reported cases in Hubei (excluding Wuhan) had a high similarity. Moreover, the spatial correlation coefficient between the newly reported cases and healthcare worker cases was 0.816 in Hubei (excluding Wuhan) on February 6, whereas that between the cumulative reported and healthcare worker cases was 0.846. The results showed that the cumulative reported cases and daily new cases were highly correlated with the

infection situation of healthcare workers in Hubei (excluding Wuhan), which indicates that the phenomenon of under-reporting had little impact on the spatial distribution of COVID-19 in Hubei (excluding Wuhan).

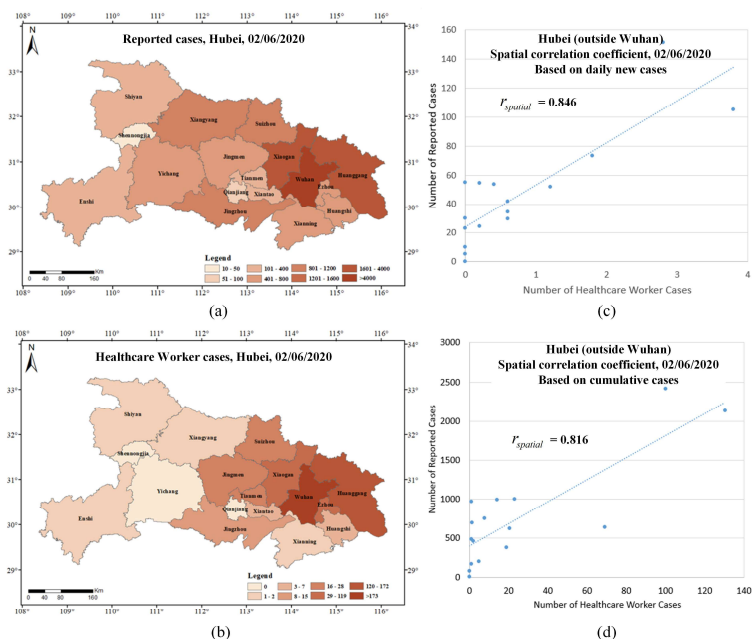


Figure 14. Spatial correlation between healthcare worker cases and reported cases in Hubei (excluding Wuhan). (a) Reported COVID-19 cases in Hubei (excluding Wuhan) on February 6, 2020; (b) healthcare worker cases in Hubei (excluding Wuhan) on February 6, 2020; (c) spatial correlation coefficient in Hubei (excluding Wuhan) on February 6, 2020, based on daily new cases; and (d) spatial correlation coefficient in Hubei (excluding Wuhan) on February 6, 2020, based on cumulative cases

As Figures 13 and 14 only show the spatial correlation between healthcare worker and reported cases at a single time node in Wuhan and Hubei (excluding Wuhan), we further demonstrate the spatial correlation changes over time in both locations in Figure 15.

The results show that the spatial correlation coefficient of daily new cases in Wuhan and Hubei (excluding Wuhan) had a certain volatility, which may have been caused by the spatial heterogeneity of the temporal lag. Secondly, the spatial correlation of new cases in Hubei (excluding Wuhan) dropped sharply from February 11 to February 29; this was because the relevant department made some corrections to the data on reported cases, which led to the decline in the spatial correlation in a short period of time. However, after February 29, the spatial correlation of new cases in Hubei (excluding Wuhan) rapidly increased and exceeded the correlation coefficient in the early stage of the epidemic.

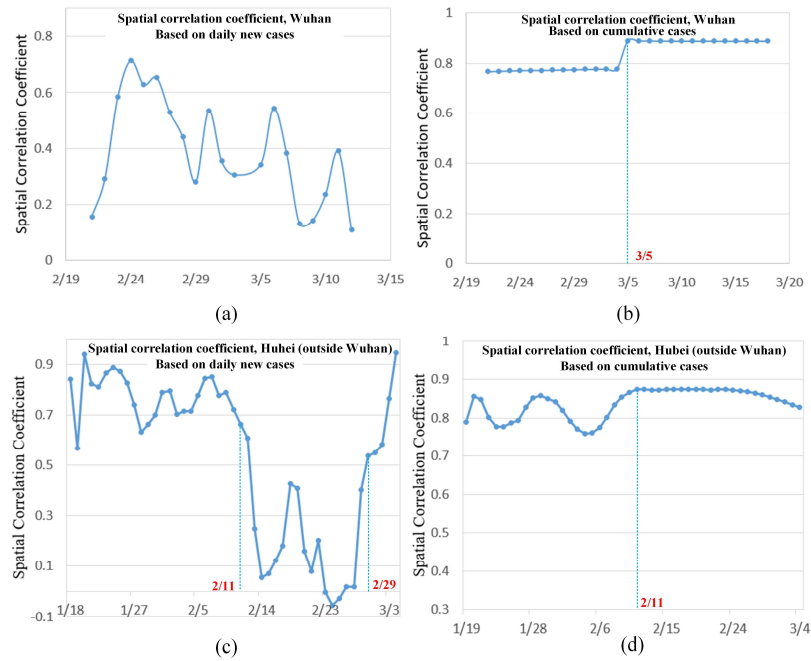


Figure 15. Changes in the spatial correlation between healthcare worker cases and under-reporting cases over time. (a) Spatial correlation coefficients in Wuhan, based on daily new cases; (b) those in Wuhan, based on cumulative cases; (c) those in Hubei (excluding Wuhan), based on daily new cases; and (d) those in Hubei (excluding Wuhan), based on cumulative cases.

Moreover, the spatial correlation coefficients of the cumulative cases in Wuhan and Hubei (excluding Wuhan) were high. Among them, the spatial correlation coefficient of cumulative cases in Wuhan increased sharply on March 5, as the Wuhan Municipal Government revised the statistical method used to obtain the information on reported cases on March 5 for improving the accuracy of the data. The spatial correlation coefficient of the cumulative cases in Hubei (excluding Wuhan) fluctuated slightly prior to February 11. This is because in the early stages of the pandemic, the under-reporting phenomenon was more prevalent. As time passed, the phenomenon of under-reporting was alleviated and the data on reported cases better reflected the spatial distribution characteristics of COVID-19.

Overall, the impact of the under-reporting phenomenon during the early stages of the pandemic was greater than that during the later stages, which was not only observed with regard to the temporal characteristics, but also in terms of daily new cases. In addition, although the number of reported cases was lower than the number of actual cases, the spatial distribution of the cumulative reported cases in Wuhan and Hubei (excluding Wuhan) still reflected the spatial pattern of COVID-19. Therefore, it is appropriate to use the data on cumulative reported cases to study the spatial distribution characteristics of COVID-19.

4.2.2 Impact of Under-reported Cases on Spatial Lag

Figure 16 shows the spatial lag of healthcare worker infection and reported cases in Wuhan and Hubei (excluding Wuhan). The results show that the spatial lag of cumulative cases had an insignificant effect on the spatial correlation in Wuhan and Hubei (excluding Wuhan).

However, the spatial lag of daily new cases had a greater effect on spatial correlation, and the effect in Wuhan was greater than that in Hubei (excluding Wuhan). To further analyze the spatial lag phenomenon quantitatively, we fixed the lag days and averaged the corresponding spatial correlation coefficients. Table 8 shows the average spatial correlation coefficients for specific lag days. The results show that the spatial correlation coefficient based on daily new cases in Wuhan increased rapidly with the increase in lag days, whereas that based on daily new cases in Hubei (excluding Wuhan) only changed slightly with the increase in lag days. This shows that daily new cases were greatly affected by under-reporting. Among them, under-reporting had a greater impact in Wuhan than in Hubei (excluding Wuhan). In addition, the spatial correlation coefficient based on the cumulative cases in Wuhan and Hubei (excluding Wuhan) changed slightly with the increase in lag days. This indicates that accumulative cases in Hubei (excluding Wuhan) and Wuhan were less affected by the under-reporting phenomenon.

Overall, the impact of under-reported cases on spatial lag was similar to the impact on spatial correlation. That is, the impact of under-reporting on the early stages of the pandemic was greater than that on the later stages, and its impact on daily new cases was greater than that on accumulative cases.

Table 8. Average spatial correlation coefficient for specific lag days

Lag days	Wuhan		Hubei (outside Wuhan)	
	Daily new cases	Cumulative cases	Daily new cases	Cumulative cases
0	0.3897	0.8117	0.5429	0.8414
1	0.3709	0.8111	0.5429	0.8420
2	0.3939	0.8106	0.5429	0.8427
3	0.4165	0.8101	0.5429	0.8439
4	0.4492	0.8096	0.5362	0.8456
5	0.4923	0.8091	0.5362	0.8475
6	0.5249	0.8085	0.5362	0.8489
7	0.5392	0.8079	0.5636	0.8495
8	0.5616	0.8072	0.5636	0.8493
9	0.5766	0.8066	0.5636	0.8486

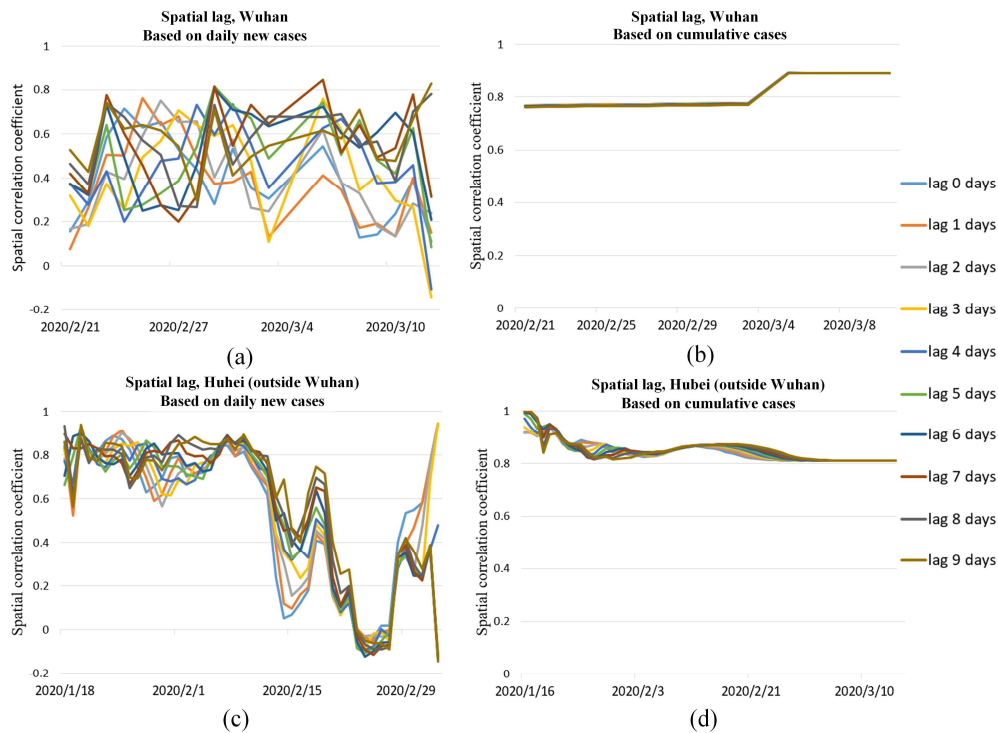


Figure 16. (a) Spatial lag phenomenon between healthcare worker cases and under-reporting cases in Wuhan, based on daily new cases; (b) those in Wuhan, based on cumulative cases; (c) those in Hubei (excluding Wuhan), based on daily new cases; and (d) those in Hubei (excluding Wuhan), based on cumulative cases.

5 Discussion and Conclusions

For the epidemic prevention and control of COVID-19, it is important to acquire a timely understanding of its spatiotemporal patterns and determine its development trend in early stage. However, under-reporting is a very common phenomenon in public health fields such as epidemiology and biomedicine. When the under-reporting phenomenon is not considered, inaccurate inferences may be produced, which will affect the judgment of decision makers (Paixão et al., 2020). Existing studies have conducted a considerable amount of work on under-reporting in data. However, few studies have explored the impact of under-reported cases on the spatiotemporal distribution of COVID-19. In this study, confirmed cases of healthcare workers were considered as an accurately small sample to analyze the impact of under-reporting on the spatiotemporal distribution of COVID-19 in Wuhan and Hubei (excluding Wuhan).

In terms of temporal characteristics, the log normal distribution was the most suitable to describe the evolution of the epidemic with time in Wuhan and Hubei (excluding Wuhan). According to the log normal distribution, the estimated peak infection time of the reported cases was 13 days later than that of the healthcare worker cases in Wuhan, and the estimated peak infection time of the reported cases was three days later than that of the healthcare worker cases in Hubei (excluding Wuhan). The estimated infection time interval of the reported cases was 15.6 days shorter than that of the healthcare worker cases in Wuhan and Hubei (excluding Wuhan). That is, the estimated peak infection time determined by reported cases lagged behind

the actual peak infection time, and the estimated time interval of infection determined using data on reported cases was smaller than the actual infection time interval. This conclusion is similar to the results obtained by Li et al. (2020), who found that the peak of the number of internet searches related to the COVID-19 outbreak occurred 10 days earlier than the peak of daily incidences in Wuhan. The occurrence of healthcare worker infections preceded the peak of internet searches, which proves the rationality of our results to a certain extent. In addition, we also analyzed the impact of under-reporting on time characteristics from the perspective of temporal correlation and temporal lag and found that the impact of under-reporting on the early onset area was greater than that on the late onset area of the epidemic, and the impact on the early stage was greater than that on the later stage. In general, the phenomenon of under-reporting had a greater impact on the estimated time characteristics of the epidemic.

Regarding spatial characteristics, the impact of the under-reporting phenomenon on daily new cases was greater than that on cumulative cases. This effect was manifested not only in the spatial correlation, but also in the spatial lag. In addition, although the number of reported cases was lower than the number of actual cases, the cumulative reported cases reflected the spatial pattern of COVID-19. For example, the spatial correlation coefficient between the cumulative reported cases and cumulative healthcare cases in Wuhan on March 6 was 0.889, whereas that between the cumulative reported cases and cumulative healthcare worker cases in Hubei (excluding Wuhan) on February 6 was 0.816; this indicated that the cumulative reported cases were highly correlated with actual infections. In general, the impact of under-reporting on the spatial distribution of COVID-19 was relatively minor. Therefore, it is feasible to use data on reported cases to study the spatial distribution characteristics of COVID-19.

The limitations of this study were as follows: (1) The coverage of healthcare worker infection data was narrow. This study only used healthcare worker infection data in China to explore the impact of under-reported cases on the spatiotemporal distribution of COVID-19 and lacks data analysis from other countries; and (2) the infection data of healthcare workers was not comprehensive. As the information on healthcare worker infections was published on the official website of the Red Cross Foundation in batches, information may continue to be published in the future, and therefore, this article may lack some of this information. In response to the above limitations, future studies should focus on collecting further data on domestic and foreign healthcare worker and patient infections to analyze the impact of under-reported cases on the spatiotemporal distribution of COVID-19 more accurately and comprehensively.

Data and codes availability statement

Data and code that support the findings of this study are available in 'figshare.com' with the identifier: <http://doi.org/10.6084/m9.figshare.13560455>

References

- Backer, J. A., Klinkenberg, D., & Wallinga, J. (2020). Incubation period of 2019 novel coronavirus (2019-nCoV) infections among travellers from Wuhan, China, 20–28 January 2020. *Eurosurveillance*, 25(5).
- Benesty, J., Chen, J., Huang, Y., & Cohen, I. (2009). Pearson correlation coefficient *Noise reduction in*

- speech processing* (pp. 1-4): Springer.
- Cabaña, A., Arratia, A., Fernández-Fontelo, A., Moriña, D., & Puig, P. (2020). *Estimation of Under-Reporting in CoVID-19 Data (in english)*.
- Chen, S., Li, Q., Gao, S., Kang, Y., & Shi, X. (2020). Mitigating COVID-19 outbreak via high testing capacity and strong transmission-intervention in the United States. *medRxiv*.
- Derrick, T. R., & Thomas, J. M. (2004). Time series analysis: the cross-correlation function. *Epidemiology Working Group for NCIP Epidemic Response, C. C. f. D. C. P.* (2020). The epidemiological characteristics of an outbreak of 2019 novel coronavirus diseases (COVID-19) in China. *Chinese Journal of Epidemiology, 41*(02), 145-151.
- Fang, Z., Yi, F., Wu, K., Lai, K., Sun, X., Zhong, N., & Liu, Z. (2020). Clinical Characteristics of Coronavirus Pneumonia 2019 (COVID-19): An Updated Systematic Review. *medRxiv*, 2020.2003.2007.20032573. doi:10.1101/2020.03.07.20032573
- Farrington, C. P., Andrews, N. J., Beale, A. D., & Catchpole, M. A. (1996). A Statistical Algorithm for the Early Detection of Outbreaks of Infectious Disease. *Journal of the Royal Statistical Society: Series A (Statistics in Society), 159*(3), 547-563. doi:<https://doi.org/10.2307/2983331>
- Fernández - Fontelo, A., Cabaña, A., Puig, P., & Moriña, D. (2016). Under - reported data analysis with INAR - hidden Markov chains. *Statistics in Medicine, 35*(26), 4875-4890.
- Foundation, C. R. C. (2020). Management rules of Chinese Red Cross Foundation ByteDance healthcare workers humanitarian relief fund (Revised Edition). Retrieved from <https://new.crcf.org.cn/article/19718>
- Gao, W., Sanna, M., Tsai, M.-K., & Wen, C. P. (2020). Geo-temporal distribution of 1,688 Chinese healthcare workers infected with COVID-19 in severe conditions—A secondary data analysis. *Plos One, 15*, e0233255. doi:10.1371/journal.pone.0233255
- Golding, N., Russell, T. W., Abbott, S., Hellewell, J., Pearson, C. A. B., van Zandvoort, K., . . . Kucharski, A. J. (2020). Reconstructing the global dynamics of under-ascertained COVID-19 cases and infections. *medRxiv*, 2020.2007.2007.20148460. doi:10.1101/2020.07.07.20148460
- Guan, W.-j., Ni, Z.-y., Hu, Y., Liang, W.-h., Ou, C.-q., He, J.-x., . . . Zhong, N.-s. (2020). Clinical Characteristics of Coronavirus Disease 2019 in China. *New England Journal of Medicine, 382*(18), 1708-1720. doi:10.1056/NEJMoa2002032
- Hu, T., Guan, W. W., Zhu, X., Shao, Y., Liu, L., Du, J., . . . Bao, S. (2020). Building an Open Resources Repository for COVID-19 Research. *Data and Information Management, 4*(3), 1–18. doi:10.2478/dim-2020-0012
- Huang, C., Wang, Y., Li, X., Ren, L., Zhao, J., Hu, Y., . . . Cao, B. (2020). Clinical features of patients infected with 2019 novel coronavirus in Wuhan, China. *The Lancet, 395*(10223), 497-506. doi:[https://doi.org/10.1016/S0140-6736\(20\)30183-5](https://doi.org/10.1016/S0140-6736(20)30183-5)
- Jia, J., Lu, X., Yuan, Y., Xu, G., Jia, J., & Christakis, N. (2020). Population Flow Drives Spatio-temporal Distribution of COVID-19 in China. *Nature, 582*(7812), 1-11.
- Justin, Lessler, and, Nicholas, Reich, and, . . . and. (2009). Incubation periods of acute respiratory viral infections: a systematic review. *Lancet Infectious Diseases*.
- Lachmann, A., Jagodnik, K. M., Giorgi, F. M., & Ray, F. (2020). Correcting under-reported COVID-19 case numbers: estimating the true scale of the pandemic. *medRxiv*. doi:10.1101/2020.03.14.20036178
- Lau, H., Khosrawipour, T., Kocbach, P., Ichii, H., Bania, J., & Khosrawipour, V. (2020). Evaluating the massive underreporting and undertesting of COVID-19 cases in multiple global epicenters.

Pulmonology. doi:<https://doi.org/10.1016/j.pulmoe.2020.05.015>

- Lauer, S. A., Grantz, K. H., Bi, Q., Jones, F. K., Zheng, Q., Meredith, H. R., . . . Lessler, J. (2020). The incubation period of coronavirus disease 2019 (COVID-19) from publicly reported confirmed cases: estimation and application. *Annals of internal medicine*, 172(9), 577-582.
- Li, C., Chen, L. J., Chen, X., Zhang, M., Pang, C. P., & Chen, H. (2020). Retrospective analysis of the possibility of predicting the COVID-19 outbreak from Internet searches and social media data, China, 2020. *Eurosurveillance*, 25(10), 2000199.
- Linton, N. M., Kobayashi, T., Yang, Y., Hayashi, K., & Nishiura, H. (2020). Incubation Period and Other Epidemiological Characteristics of 2019 Novel Coronavirus Infections with Right Truncation: A Statistical Analysis of Publicly Available Case Data. *Journal of Clinical Medicine*, 9(2), 538-.
- Liu, Q., Sha, D., Liu, W., Houser, P., Zhang, L., Hou, R., . . . Hu, T. (2020). Spatiotemporal Patterns of COVID-19 Impact on Human Activities and Environment in Mainland China Using Nighttime Light and Air Quality Data. *Remote Sensing*, 12(10), 1576.
- Mace, R. D., Minta, S. C., Manley, T. L., & Aune, K. E. (1994). Estimating grizzly bear population size using camera sightings. *Wildlife Society Bulletin (1973-2006)*, 22(1), 74-83.
- Paixão, B., Baroni, L., Salles, R., Escobar, L., de Sousa, C., Pedroso, M., . . . Ogasawara, E. (2020). Estimation of COVID-19 under-reporting in Brazilian States through SARI. *arXiv preprint arXiv:2006.12759*.
- Prado, M. F. D., Antunes, B. B. D. P., Bastos, L. D. S. L., Peres, I. T., & Bozza, F. A. (2020). Analysis of COVID-19 under-reporting in Brazil. *Revista Brasileira de Terapia Intensiva(AHEAD)*.
- Saberi, M., Hamedmoghadam, H., Madani, K., Dolk, H. M., Morgan, A. S., Morris, J. K., . . . Khoshnood, B. (2020). Accounting for Underreporting in Mathematical Modeling of Transmission and Control of COVID-19 in Iran. *Frontiers in Physics*, 8(289). doi:10.3389/fphy.2020.00289
- Shen, M., Peng, Z., Xiao, Y., & Zhang, L. (2020). Modelling the epidemic trend of the 2019 novel coronavirus outbreak in China. *bioRxiv*.
- Smid, S. C., McNeish, D., Miočević, M., & van de Schoot, R. (2020). Bayesian versus frequentist estimation for structural equation models in small sample contexts: A systematic review. *Structural Equation Modeling: A Multidisciplinary Journal*, 27(1), 131-161.
- Tang, B., Wang, X., Li, Q., Bragazzi, N. L., Tang, S., Xiao, Y., & Wu, J. (2020). Estimation of the transmission risk of the 2019-nCoV and its implication for public health interventions. *Journal of Clinical Medicine*, 9(2), 462.
- Unkel, S., Farrington, C. P., Garthwaite, P. H., Robertson, C., & Andrews, N. (2012). Statistical methods for the prospective detection of infectious disease outbreaks: a review. *Journal of the Royal Statistical Society: Series A (Statistics in Society)*, 175(1), 49-82.
- Wang, S. Y., Liu, Y., Struthers, J., & Lian, M. (2020). Spatiotemporal Characteristics of COVID-19 Epidemic in the United States. *Clinical infectious diseases*, ciaa934. doi:10.1093/cid/ciaa934
- Yang, C., Sha, D., Liu, Q., Li, Y., Lan, H., Guan, W. W., . . . Thompson, J. H. (2020). Taking the pulse of COVID-19: A spatiotemporal perspective. *International Journal of Digital Earth*, 1-26.